# General Adaptive Neighborhood Image Processing. Part II: Practical Applications Issues

Johan Debayle, Jean-Charles Pinoli

# General Adaptive Neighborhood Image Processing
## Part II: Practical Application Examples

JOHAN DEBAYLE (debayle@emse.fr) and JEAN-CHARLES PINOLI† (pinoli@emse.fr)
*Ecole Nationale Supérieure des Mines de Saint-Etienne, France*

Submitted: March 17, 2005. Revised form: November 3, 2005 and January 23, 2006.
Regular Paper, submitted to: **Journal of Mathematical Imaging and Vision**

**Abstract.** The so-called General Adaptive Neighborhood Image Processing (GANIP) approach is presented in a two parts paper dealing respectively with its theoretical and practical aspects.
The General Adaptive Neighborhood (GAN) paradigm, theoretically introduced in Part I [20], allows the building of new image processing transformations using context-dependent analysis. With the help of a specified *analyzing criterion*, such transformations perform a more significant spatial analysis, taking intrinsically into account the local radiometric, morphological or geometrical characteristics of the image. Moreover they are consistent with the physical and/or physiological settings of the image to be processed, using *general linear image processing* frameworks.
In this paper, the GANIP approach is more particularly studied in the context of Mathematical Morphology (MM). The structuring elements, required for MM, are substituted by GAN-based structuring elements, fitting to the local contextual details of the studied image. The resulting morphological operators perform a really spatially-adaptive image processing and notably, in several important and practical cases, are connected, which is a great advantage compared to the usual ones that fail to this property.
Several GANIP-based results are here exposed and discussed in image filtering, image segmentation, and image enhancement. In order to evaluate the proposed approach, a comparative study is as far as possible proposed between the adaptive and usual morphological operators. Moreover, the interests to work with the Logarithmic Image Processing framework and with the 'contrast' criterion are shown through practical application examples.

**Keywords:** General Adaptive Neighborhoods, Image Processing Frameworks, Intrinsic Spatially-Adaptive Analysis, Mathematical Morphology, Nonlinear Image Representation

### Table of Contents



† corresponding author

## Part II: Practical Application Examples



### Abbreviations

| | | |
|---|---|---|
| AN | : | Adaptive Neighborhood |
| ANIP | : | Adaptive Neighborhood Image Processing |
| ASE | : | Adaptive Structuring Element |
| ASF | : | Alternating Sequential Filter |
| CLIP | : | Classical Linear Image Processing |
| IP | : | Image Processing |
| GAN | : | General Adaptive Neighborhood |
| GANIP | : | General Adaptive Neighborhood Image Processing |
| GANMM | : | General Adaptive Neighborhood Mathematical Morphology |
| GLIP | : | General Linear Image Processing |
| LIP | : | Logarithmic Image Processing |
| LRIP | : | Log-Ratio Image Processing |
| MHIP | : | Multiplicative Homomorphic Image Processing |
| MM | : | Mathematical Morphology |
| SE | : | Structuring Element |

This paper deals with intensity images, that is to say image mappings defined on a spatial support $D$ in the Euclidean space $\mathbb{R}^2$ and valued into a gray tone range, which is a positive real numbers interval.
The first occurrence of a specific and/or important term will appear in italics.

## 1. Introduction

The Adaptive Neighborhood (AN) paradigm allows the building of new image processing transformations using context-dependent analysis. Such transforms are no longer spatially invariant, but vary over the whole image with ANs as adaptive operational windows, taking intrinsically into account the local image features. This AN concept is largely extended [20], using well-defined mathematical concepts, to that of General Adaptive Neighborhood (GAN) in two main ways.Firstly, an *analyzing criterion* is added within the definition of the ANs in order to consider the radiometric, morphological or geometrical characteristics of the image, allowing a more significant spatial analysis. Secondly *general linear image processing* (GLIP) frameworks are introduced in the GAN approach, using concepts of abstract linear algebra, so as to develop operators that are consistent with the physical and/or physiological settings of the image to be processed. The so-called General Adaptive Neighborhood Image Processing (GANIP) approach is more particularly studied [20] in the context of Mathematical Morphology (MM). The structuring elements, required for MM, are substituted by GAN-based structuring elements, fitting to the local contextual details of the studied image. The resulting transformations perform a really spatially-adaptive image processing, in an intrinsic manner, that is to say without a priori knowledge of the image structures. Moreover, in several important and practical cases, the GANIP-based morphological operators are connected, which is an overwhelming advantage compared to the usual ones which fail to this property. The theoretical aspects of the General Adaptive Neighborhood Image Processing (GANIP) approach are presented in [20].
In this paper, GANIP-based practical application examples, and more particularly in the context of MM, are successively exposed in image filtering, image segmentation, and image enhancement. In order to evaluate the proposed approach, a comparative study is as far as possible proposed between the adaptive and usual morphological operators. The results achieved from GAN-based morphological operators take into account specified and appropriate general adaptive neighborhood sets.

## 2. Image Filtering

Most of the time, image filtering is a necessary preliminary step in image pre-processing, such as denoising, restoration, pre-segmentation, enhancement, sharpening, brightness correction, ... [31]. GANIP-based filtering [19] allows such transformations to be defined. More particularly, Section 2 addresses image filtering in the respective noise-free and noisy conditions, highlighting the generalized aspect of the GANIP approach. Thereafter, Sections 3. and 4. show respectively the advantages of the GAN-based morphological filters in image pre-segmentation and image enhancement.

### *2.1. Noise-free image filtering*

An illustration of GANIP-based filtering using adaptive opening-closings (Eq. 53 in [20]) is exposed in Figure 1 on a part of the 'Moon' image. The process is performed within the CLIP, MHIP, LRIP and LIP frameworks (Subsection 2.4 in [20]) selected for the *space of criterion mappings*, denoted respectively $\mathcal{C}_{CLIP}$, $\mathcal{C}_{MHIP}$, $\mathcal{C}_{LRIP}$ and $\mathcal{C}_{LIP}$. These spaces will be shortly named *criterion spaces* in the following. The homogeneity tolerance $m_{\bigcirc}$, used as parameter in the ASEs (Paragraph 4.3.1 in [20]), is valued within $\mathcal{C}_{CLIP}$ from a positive real value $m$. In order to generalize this parameter to any GLIP framework, the value of the homogeneity tolerance, denoted $m_{\bigcirc}$, is obtained from $m \in \mathbb{R}^+$ added up to the real value corresponding to the neutral element $0_{\bigcirc}$ of the considered framework:

$$m_{\bigcirc} = 0_{\bigcirc} + m \tag{1}$$

However, the value $m \in \mathbb{R}^+$ should be chosen such as $0_{\bigcirc} + m$ belongs to the positive intensity value range $E^{\oplus}$ (Tab.I in [20]).
In this way, the homogeneity tolerance given in the CLIP, MHIP, LRIP or LIP framework is respectively valued as:

$$\mathcal{C}_{CLIP} \ : \ m = 0 + m \tag{2}$$

$$\mathcal{C}_{MHIP} \ : \ m_{\square} = 1 + m \tag{3}$$

$$\mathcal{C}_{LRIP} \ : \ m_{\lozenge} = \frac{M}{2} + m \tag{4}$$

$$\mathcal{C}_{LIP} \ : \ m_{\triangle} = 0 + m \tag{5}$$

Two positive real values are considered, in Figure 1, for the homogeneity tolerance: $m = 1$ and $m = 20$. From this point, the equivalent corresponding values within the spaces $\mathcal{C}_{CLIP}$, $\mathcal{C}_{MHIP}$, $\mathcal{C}_{LRIP}$ and $\mathcal{C}_{LIP}$ of criterion mappings, are inferred from Equations (2)-(5).
Concerning the second parameter of the ASEs, the analyzing criterion is the 'luminance'.

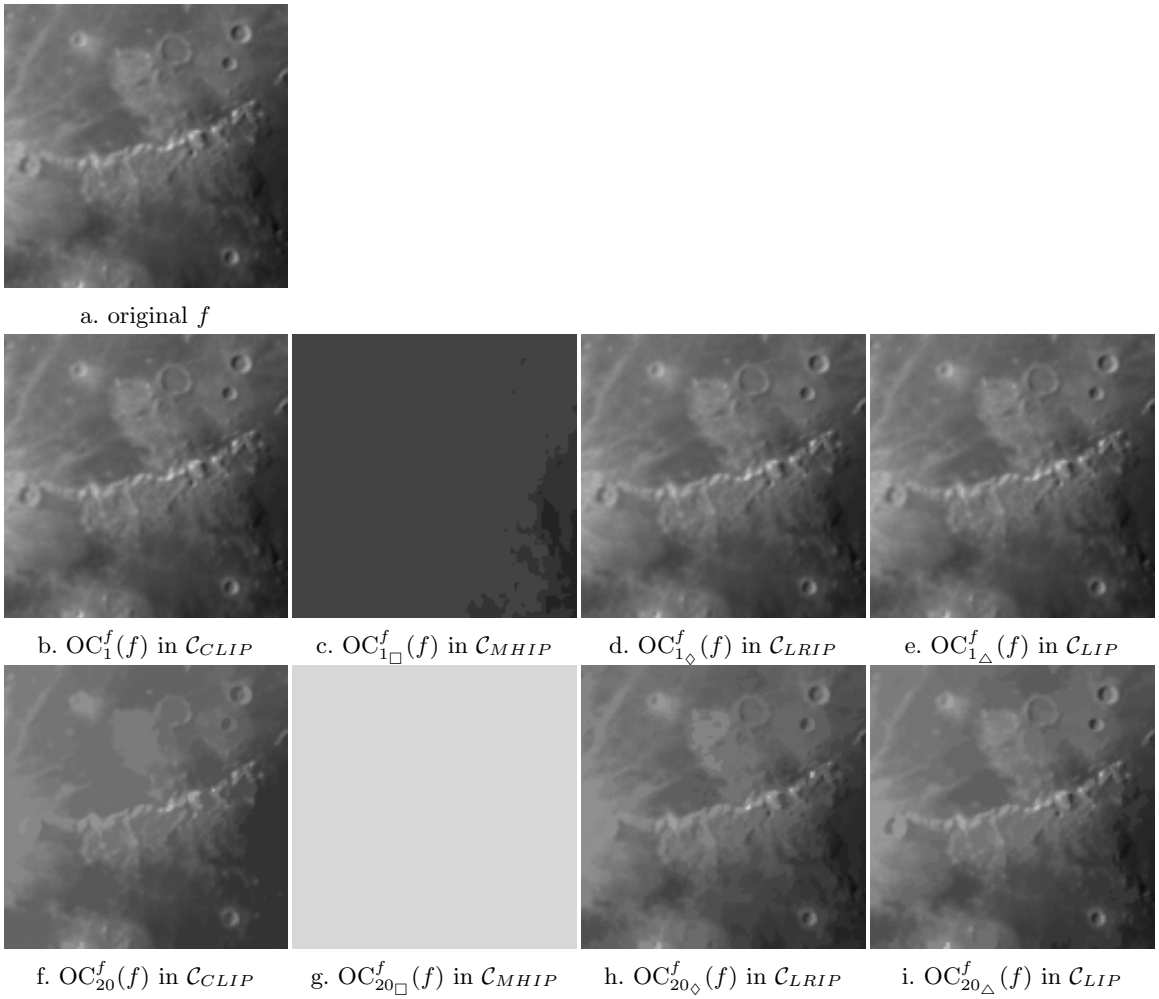

a. original $f$

b. $\mathrm{OC}_{1}^{f}(f)$ in $\mathcal{C}_{CLIP}$ c. $\mathrm{OC}_{1_{\square}}^{f}(f)$ in $\mathcal{C}_{MHIP}$ d. $\mathrm{OC}_{1_{\lozenge}}^{f}(f)$ in $\mathcal{C}_{LRIP}$ e. $\mathrm{OC}_{1_{\triangle}}^{f}(f)$ in $\mathcal{C}_{LIP}$

f. $\mathrm{OC}_{20}^{f}(f)$ in $\mathcal{C}_{CLIP}$ g. $\mathrm{OC}_{20_{\square}}^{f}(f)$ in $\mathcal{C}_{MHIP}$ h. $\mathrm{OC}_{20_{\lozenge}}^{f}(f)$ in $\mathcal{C}_{LRIP}$ i. $\mathrm{OC}_{20_{\triangle}}^{f}(f)$ in $\mathcal{C}_{LIP}$

*Figure 1.* GANIP-based filtering using adaptive opening-closings $\mathrm{CO}_{m}^{f}$ on a part of the 'Moon' [a] image $f$. The processing is illustrated within the CLIP (first column except image [a]), MHIP (second column), LRIP (third column) and LIP (fourth column) frameworks selected for the space of criterion mappings. Two distinct values (in their respective framework) of the homogeneity tolerance, $m = 1$ (second line) and $m = 20$ (third line), are exposed to point out the effects induced by this intensity-based parameter.

The filtering process performs a smoothing all the more strong so the value of the parameter $m$ increases. The original 'Moon' image $f$ (Figure 1.a) is already damaged for $m = 1$ (Figure

1.c) within the criterion space $\mathcal{C}_{MHIP}$, whose IP framework, MHIP, is consequently not adapted. Next, $\mathcal{C}_{CLIP}$ and $\mathcal{C}_{CLIP}$ generate several drawbacks, removing (Figure 1.f,h) over quickly significant details such as the 'crater' located in the left-center of the original image. Finally, the LIP framework appears to be the most appropriate to this filtering process, allowing the original image to be smoothed without damaging its features (Figure 1.i).

### *2.2. Noisy image filtering*

The adaptive filters using the elementary GANs work well if the processed images are noise free or a bit corrupted (Fig. 1). In the presence of impulse noise, such as 'salt and pepper' noise, the GANs need to be combined to provide efficient filtering operators. Indeed, the elementary GAN of a corrupted point by such a noise does not generally fit to the 'true' region of which it belongs, for any homogeneity tolerance $m_{\bigcirc}$.
Consequently, a specific kind of GANs, the *Combined General Adaptive Neighborhoods* (C-GANs) denoted $Z^f_{m_{\bigcirc}}(.)$, are introduced to enable images corrupted by such a noise to be restored. They are built by combination (with the set union) of the W-GANs $\{V^f_{m_{\bigcirc}}(y)\}_{y\in D}$ using the luminance criterion. Explicitly, the C-GANs are defined as following:

**Definition 1 (Combined General Adaptive Neighborhoods).**
$\forall (m_{\bigcirc}, f, x) \in E^{\oplus} \times \mathcal{I} \times D$

$$Z^f_{m_{\bigcirc}}(x) = \begin{cases} \bigcup\limits_{y\in B_1(x)} \{V^f_{m_{\bigcirc}}(y)\} & \text{if } A(V^f_{m_{\bigcirc}}(x)) \leq \pi * q^2 \\ V^f_{m_{\bigcirc}}(x) & \text{otherwise} \end{cases} \tag{6}$$

*where $B_1(x)$ refers to the disk of radius 1 centered to $x$, and $A(X)$ to the area of $X$, and $q$ to a real number.*

The value of the parameter $q$ has been visually tuned to 0.6. A specific study should be lead so as to find an automatic way of picking this parameter (probably linked to the percentage of damaged points in the image). These C-GANs allow to detect the 'true' neighborhood of a corrupted point $x$, with the help of the area of its W-GAN $V^f_{m_{\bigcirc}}(x)$.

**Remark 2.** *It is obviously possible to introduce other combined GANs relating to the specific kind of noise to be removed.*

Several operators, based on these C-GANs, could be introduced. Figure 2 illustrates a restoration process using median filtering [31]. When performing median filtering, the output value of each image point to be processed is determined by the median value of all points in a selected neighborhood (isotropic centered disk, GAN, ...). The median value $q$ of a neighboring population (set of points in a neighborhood) is this value for which half of the population has smaller values than $q$, and the other half has larger values than $q$. The classical median filter, denoted $Med_r$, using a disk of radius $r$ and the adaptive filters using W-GANs ($V\text{-}Med^g_{20}(.)$) and C-GANs ($Z\text{-}Med^g_{20}(.)$), with the luminance criterion and the parameter 20 as homogeneity tolerance in the CLIP framework, are applied on the 'Lena' image $g$, which is corrupted by a salt and pepper noise.

The results show the necessity to combine the W-GANs to perform a significant filtering. In addition, the median filter (using the C-GANs) supplies a better result than the usual median filter (using an isotropic disk). Indeed, the edges are damaged with the classical approach (blur occurs around the eyes and the hairs), contrary to the GANIP one.

a. noise-free image $f$

b. noisy image $g$

c. $Med_1(g)$

d. $V\text{-}Med^g_{20}(g)$

e. $Z\text{-}Med^g_{20}(g)$

*Figure 2.* Image restoration. Image [a] is corrupted with a 10% salt and pepper noise [b]. Median filtering is used to filter the noisy image: usual filtered image [c] with a disk of radius 1 as operational window, adaptive median filtered image [d] with $V^g_{20}(.)$ GANs and adaptive filtered image [e] with $Z^f_{20}(.)$. The most efficient denoising is supplied by the C-GANs filter.

The GANIP-based morphological filters are then used as preliminary processes generally required in image segmentation.

## 3. Image Segmentation

The segmentation of an intensity image can be defined as its *partition* (in fact the partition of the spatial support $D$) into different connected regions, each having certain properties. From a mathematical point of view, the segmentation is well-defined as follow:
the *segmentation* [31] of an image $f \in \mathcal{I}$ is a partition of its definition domain $D$ into $n$ disjoint nonempty subsets $R_1, \ldots, R_n$, called regions, such that the union of all subsets equals $D$:

$$(D = \cup_{i=1}^{n} R_i) \text{ and } (\forall i \neq j \; R_i \cap R_j = \emptyset) \tag{7}$$

In this paper, the segmentation process is based on a morphological transformation called *watershed* [4] and a GANIP-based decomposition process [20].

### *3.1. Recalls on watershed*

The watershed transformation is now well recognized as being a fundamental step in many powerful morphological segmentation processes [5, 62]. It has been made computationally practical thanks to a fast technique presented by Vincent and Soille [106]. Watershed analysis (Fig. 3) subdivides the image, considered as a topographic surface, into low-gradient *catchment basins* surrounded by high-gradient *watersheds*. A catchment basin consist of an homogeneous set of points that are all connected, through a path, to the same minimun altitude point. The watersheds are made up of connected points exhibiting local maxima in gradient magnitude; to achieve a final segmentation, these points are typically absorbed into adjacent catchment basins.

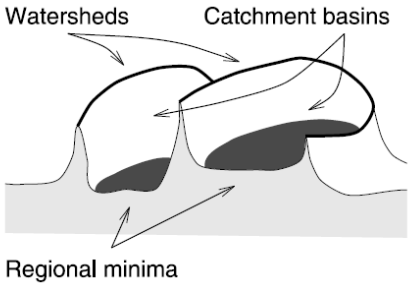


*Figure 3.* Watershed segmentation: considering the image as a topographic surface, the flooding of its regional minima, while preventing the merging of the waters coming from different sources, partitions the image into two different sets: the catchment basins and the watersheds.

In order to produce a segmentation into meaningful regions, the input image is generally transformed to output a so-called *segmentation function*, on which the watershed transformation is applied. In practice, the gradient image is often used as segmentation function, since the catchment basins should theoretically correspond to the homogeneous gray level regions of the image, and the watersheds to the discontinuities of the image.

### *3.2. Usefulness of GANIP-based Filtering*

Nevertheless, a direct computation of the watershed on the gradient image generally creates an over-segmentation which is due to the presence of spurious minima. This problem is overcome by a GANIP-based *decomposition* process to decrease the number of minima, and consequently the number of segmented regions. Indeed, the GAN filters enable to smooth the image without

damaging the transitions, thanks to their connectivity property [20].
In the following of this section, four examples will be exposed and illustrated.

### *3.3. Pyramidal Segmentation with Alternating Sequential Filters*

The aim of this first application example (Fig. 4) is to produce a multiscale segmentation of the 'Lena' image, based on a decomposition process using GAN-based and non-adaptive *pyramidal operators* [93] whose definition is below-mentioned.

**Definition 3 (Pyramid of Operators).**
*A pyramid of operators* $\{\psi_\lambda\}_{\lambda\in\mathbb{N}}$ *from* $\mathcal{I}$ *into* $\mathcal{I}$*, is a collection depending on a positive parameter* $\lambda \in \mathbb{N}$*, called the level, so that:*

$$\forall(\lambda,\mu)\in\mathbb{N}^2 \quad \lambda\geq\mu\geq 0 \quad \exists\nu\in\mathbb{N}\,|\,\nu\geq\mu\Rightarrow\psi_\nu\psi_\mu=\psi_\lambda \tag{8}$$

This pyramid of operators generates a *pyramidal decomposition* (Def. 4) of any image $f \in \mathcal{I}$.

**Definition 4 (Pyramidal Decomposition).**
*A pyramidal decomposition of an image* $f \in \mathcal{I}$ *consists in a collection* $\{\psi_\lambda(f)\}_{\lambda\in\mathbb{N}}$ *of images belonging to* $\mathcal{I}$*, decomposed at different resolution levels* $\lambda \in \mathbb{N}$*, using a 'pyramid of operators'* $\{\psi_\lambda\}_{\lambda\in\mathbb{N}}$.

In Figure 4, the considered pyramid of operators, applied on the original 'Lena' image, is a family of Alternating Sequential Filters (ASF), which satisfy the property (8). These operators then generate a pyramidal decomposition, filtering the original image to avoid an over-segmentation (Fig. 4.e.). Indeed, the original image is smoothed all the more strong so the ASF order increases. In this way, the number of minima of the segmentation function, and consequently the number of regions of the resulting segmentation, decreases.

At each pyramid level $\lambda \in \mathbb{N}$, the process of the considered pyramidal segmentation (Fig. 4) is achieved in three consecutive steps:

1. the original image $f$ is morphologically filtered with an ASF of order $\lambda$,
2. the morphological gradient, denoted $MG$, is computed on the resulting filtered image,
3. finally, the watershed transformation, denoted $Wat$, is completed on this segmentation function.

The operator denoted $Seg$ designates the two last steps of this segmentation process, therefore denoted $Wat \circ MG$, i.e. the morphological gradient followed by the watershed transformation.
In this application example, multiscale segmentation processes, using GAN-based and classical ASFs, are compared. Note that $\text{ASFCO}_{m,r}$ (resp. $\text{ASFCO}^f_{m,n}$ (Eq. 64 in [20])) represents the usual (resp. adaptive) alternating (closing-opening) sequential filter of order $n$ using the disk of radius $r$ centered in $x$, denoted $B_r(x)$, as usual SE (resp. using the ASEs $\{N^f_m(x)\}_{x\in D}$ (Eq. 34 in [20]), computed with the 'luminance' criterion in the CLIP framework). About the spatial parameter $r$ and the intensity-based parameter $m$, they are fixed to $r = 1$ for the disk radius of usual SEs, and $m = 5$ for the homogeneity tolerance of adaptive SEs. For $n$, three filtering orders are used both for GAN-based and usual ASFs: $n = 4, 7, 10$, in order to show different levels of the pyramidal segmentation.

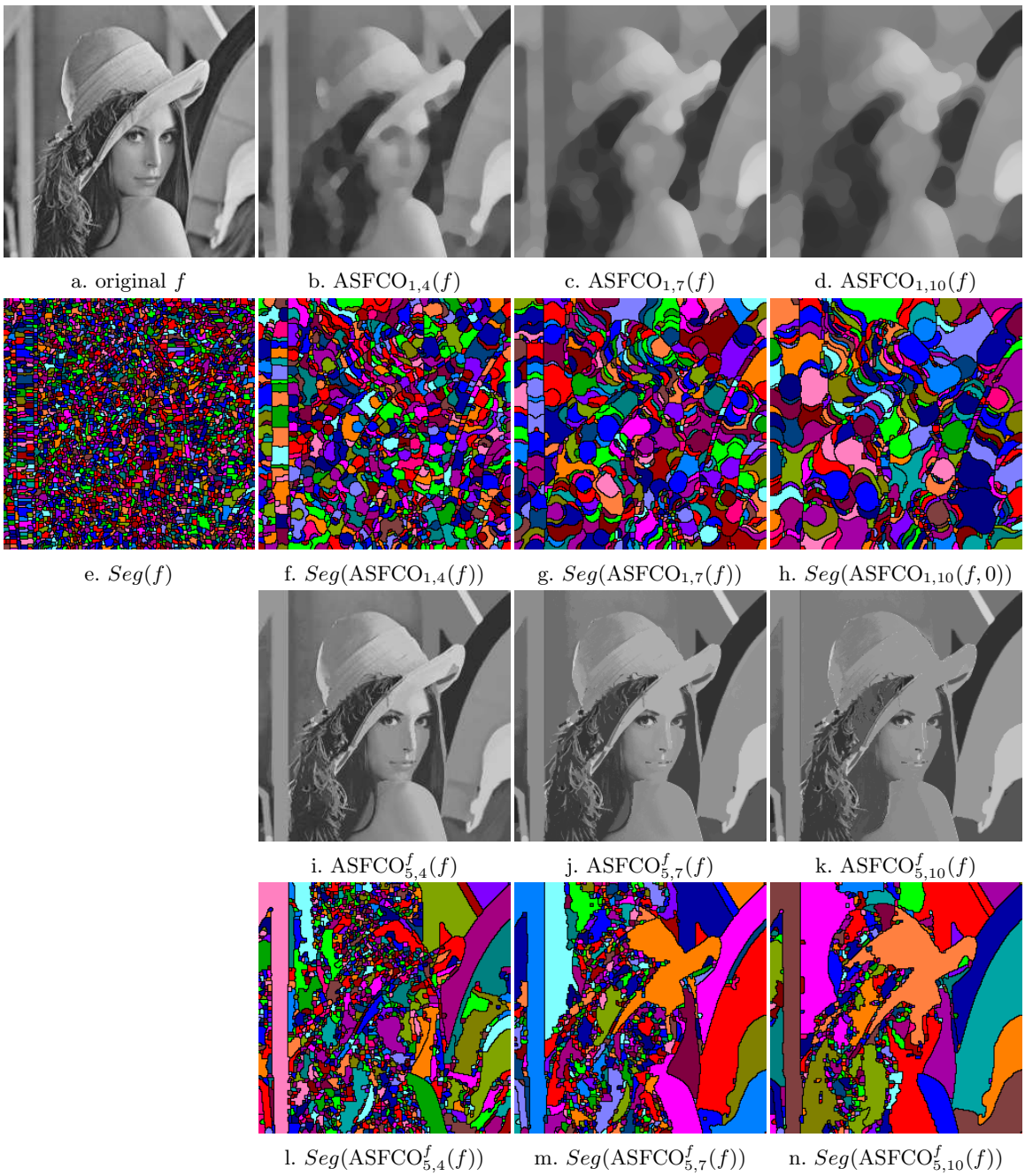


*Figure 4.* Pyramidal segmentation of the 'Lena' [a] image. First, the original image is decomposed using classical [b-d] and adaptive [i-k] alternating sequential filters. Secondly, the morphological gradient followed by the watershed transformation, denoted $Seg$, is computed on the decomposed images as segmentation functions, achieving respectively the images [f-h] and [l-n], for the non-adaptive MM-based and GANMM-based approach. The original image is decomposed so as to avoid an over-segmentation [e]. The GANIP approach provides a better segmentation taking into account the local multiscale features of the original image.

Therefore, Figure 4 shows that the GANMM-based approach overcomes the non-adaptive MM-based one. Indeed 'Lena' is all the more distinguishing with the segmentation achieved by the adaptive filters so the filtering order $n$ increases, while it's entirely impossible with the classical corresponding approach. Thus, these results highlight the importance of connectivity of the GANMM-based operators $f \mapsto \mathrm{ASFCO}^f_{m,n}(f)$ (Rem. 20 in [20]). It is an overwhelming advantage, contrary to the corresponding non-adaptive ones $f \mapsto \mathrm{ASFCO}_{m,n}(f)$ that fail to this

property. The 'Lena' image is simplified in producing flat zones while preserving the contour information. Moreover, the level of the pyramid is intrinsically dependent on the local structures of the image. Consequently, the GANIP-based operators perform a more significant decomposition than the usual ones, taking into account the multiscale topological characteristics.

### *3.4. Hierarchical Pyramidal Segmentation with Adaptive Sequential Closings*

This subsection introduces a multiscale segmentation illustrated on Figure 5, using a pyramid of connected operators, applied on the 'Tools' test image (Fig. 5.a). Such a pyramid of connected operators generates a *hierarchical pyramidal decomposition*:

**Definition 5 (Hierarchical Pyramidal Decomposition).**
*A hierarchical pyramidal decomposition of an image $f \in \mathcal{I}$ is a collection $\{\psi_\lambda(f)\}_{\lambda\in\mathbb{N}}$ of images belonging to $\mathcal{I}$, decomposed at different resolution levels $\lambda \in \mathbb{N}$, using a pyramid of connected operators $\{\psi_\lambda\}_{\lambda\in\mathbb{N}}$.*

The resulting *hierarchical pyramidal segmentation* is more relevant than a pyramidal segmentation (Subsection 3.3). Indeed, if the set of connected operators $\{\psi_\lambda\}$ creates a pyramid satisfying the property (8), then the flat zones of $\psi_\lambda$ increase with the parameter $\lambda$ [93]. It means that the flat zones are merged. It enables the structures of image to be more suitably analyzed and linked across levels of the pyramid.

In this example, the pyramid is generated with a set of GAN filters: the adaptive sequential closings $\{\mathrm{C}^f_{m,p}\}_p$ (Eq. 59 in [20]) using the adaptive SEs $N^f_m(x)$ (Eq. 34 in [20]) computed with the 'luminance' criterion in the CLIP framework. These filters are connected and satisfy the property (8), since it is a size distribution [20]. Consequently, the collection of adaptive sequential closings $\{\mathrm{C}^f_{m,p}\}_p$ defines a pyramid of connected operators, necessary to perform a hierarchical pyramidal segmentation.

In this way, at each level $p$ of the pyramid, the segmentation process is achieved in three consecutive steps:

1. the original image is filtered with an adaptive sequential closing of order $p$,
2. the morphological gradient, denoted $MG$, is computed on the filtered image,
3. finally, the watershed transformation, denoted $Wat$, is completed on this segmentation function.

The operator denoted $Seg$ designates the two last steps of this segmentation process, therefore denoted $Wat \circ MG$, i.e. the morphological gradient followed by the watershed transformation.

Concerning the parameter $p$ of the GAN filters, three filtering orders have been used, $p = 5, 15, 25$, in order to show different levels of the resulting hierarchical pyramid. About $m$, it has been selected to the real value 4 by tuning these techniques so that they produce resulting segmented images that are visually the most satisfying.

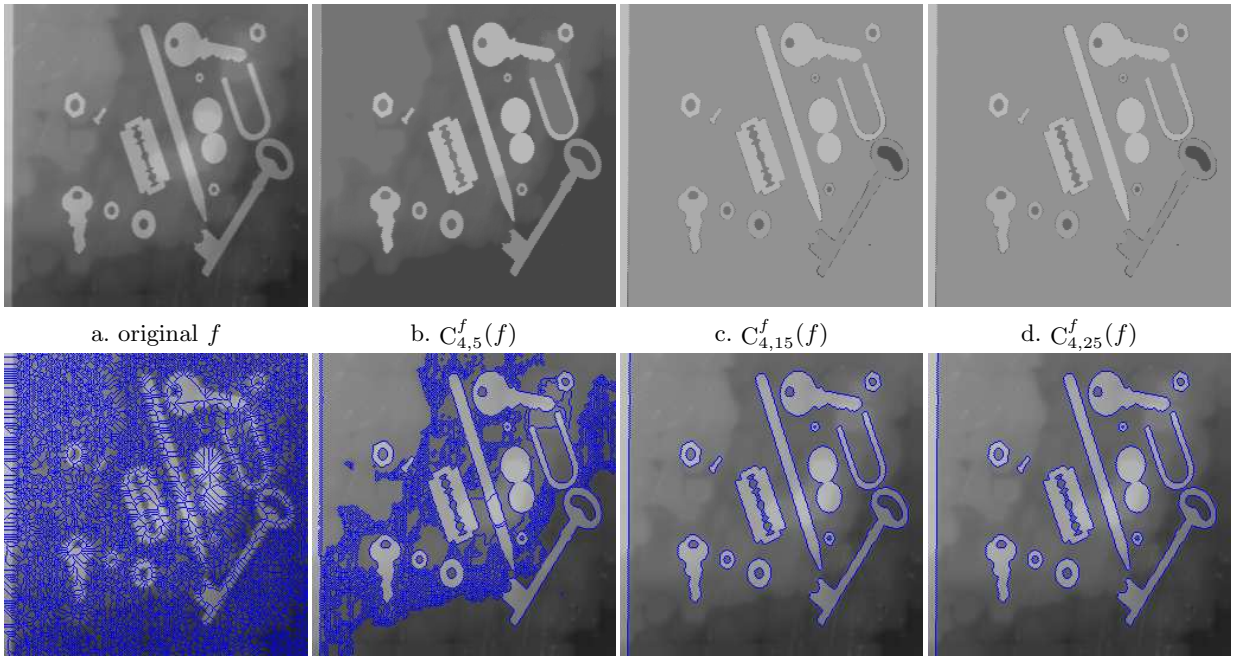

a. original $f$ b. $\mathrm{C}^f_{4,5}(f)$ c. $\mathrm{C}^f_{4,15}(f)$ d. $\mathrm{C}^f_{4,25}(f)$

e. $Seg(f)$ f. $Seg(\mathrm{C}^f_{4,5}(f))$ g. $Seg(\mathrm{C}^f_{4,15}(f))$ h. $Seg(\mathrm{C}^f_{4,25}(f))$

*Figure 5.* Hierarchical pyramidal segmentation of the 'Tools' [a] image. First, the original image is decomposed using adaptive sequential closing filters [b-d]. Secondly, the morphological gradient followed by the watershed transformation, denoted *Seg*, is computed on the decomposed images as segmentation functions, achieving the images [f-h]. The original image is decomposed so as to avoid an over-segmentation [e]. The process $Seg(\mathrm{C}^f_{4,n}(f))$ provides a well-accepted segmentation for $n \geq 15$ [g,h].

The resulting hierarchical segmentation supplies nested partitions of the original image inducing a graph representation [93, 103]. Thereafter, the process $\mathrm{C}^f_{4,n}$ supplies the expected result for $n = 15$ or $n > 15$. Indeed, this operator is saturated from this value : $\forall n > 15 \quad \mathrm{C}^f_{4,n} = \mathrm{C}^f_{4,15}$. This characteristic should be studied, promising relevant topological properties.

Moreover, the resulting hierarchical segmentation, where flat zones are nested, is achieved without any operators by reconstruction [16] that are generally used in classical methods.

**Remark 6.** *The filters by reconstruction require geodesic transformations to define connected operators, which are traditionally used for this kind of multiscale segmentation [86, 93, 103]. So, the connectivity characteristic of the GANMM-based operators [20] is an overwhelming advantage: all operators built by composition or combination with the supremum and the infimum of the adaptive dilation and erosion, thus define connected operators.*

### *3.5. Segmentation with Alternating Filters*

A real example in image segmentation is here presented (Fig. 6) on a metallurgic grain boundary image. The goal of the application is to detect the boundaries of the grains. It will allow metallurgists to get a quantitative analysis of the grains. Several methods, addressing this problem, have ever been exposed. For example, Chazallon and Pinoli [11] proposed an efficient approach based on the residues of alternating sequential filters. Nevertheless, the method still presents few drawbacks for complex images: its inability to remove some artifacts and to preserve disconnected grain boundaries. On the whole, the published methods need most of the time advanced processes and metallographically relevant and tractable a priori knowledges, requiring expert intervention.

In this application example, a simple segmentation method resulting from two steps is proposed:

1. a decomposition process, through non-adaptative MM-based and GANMM-based closing-openings, is applied on the original image,

2. the watershed transformation is then computed on these segmentation functions.

This approach does not require a gradient operator. Indeed, seeing that the crest lines of the original image fit with the narrow grain boundaries, the watershed transformation, denoted $Wat$, is directly computed on filtered images (processed with closing-openings) in order to avoid an over-segmentation seen in Figure 6.e. The segmentation function is then the filtered image, without using any gradient operators.

A comparison between the GANMM-based approach [20] and the corresponding MM-based one is performed through the filtering process.
Note that $\mathrm{CO}_r$ (resp. $\mathrm{CO}_m^f$) represents the usual closing-opening (resp. the adaptive closing-opening (Eq. 54 in [20])) using the disk of radius $r$ centered in $x$, denoted $B_r(x)$, as usual SE (resp. using the ASEs $\{N_m^f(x)\}_{x\in D}$ (Eq. 34 in [20]), computed with the 'luminance' criterion in the CLIP framework).
For each approach, three parameters have been fixed: $r = 1, 2, 3$ for the radius of the usual SEs, and $m = 10, 20, 30$ for the homogeneity tolerance of the adaptive SEs.

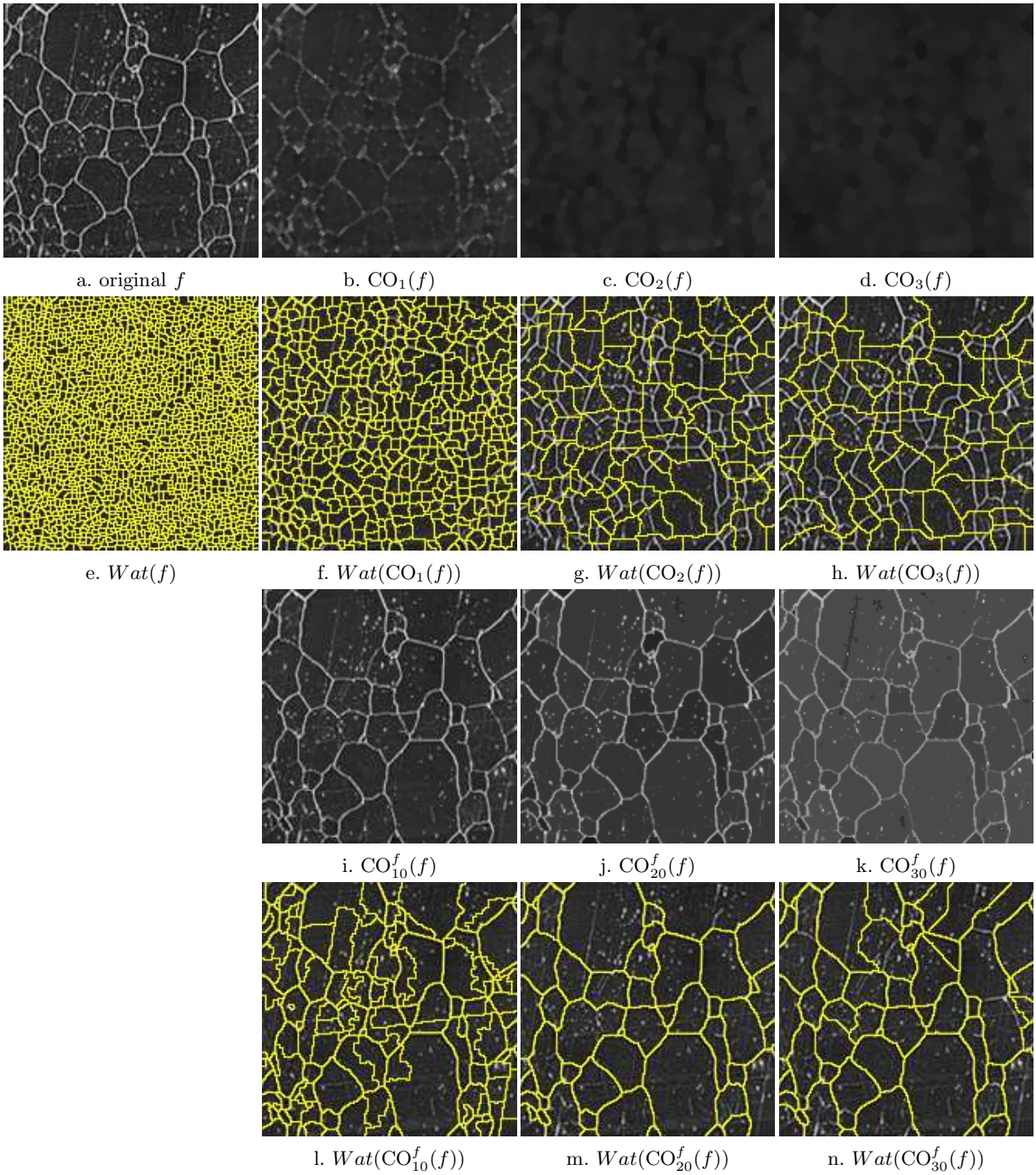


*Figure 6.* Segmentation of a real metallurgic grain boundaries [a] image. Pyramidal segmentation of the original [a] image. First, the original image is decomposed using classical [b-d] and adaptive [i-k] closing-openings. Secondly, the watershed transformation, denoted $Wat$, is computed on the decomposed images as segmentation functions, achieving respectively the images [f-h] and [l-n], for the non-adaptive MM-based and GANIP approach. The original image is decomposed to avoid an over-segmentation [e]. The adaptive approach provides a well-accepted segmentation reached for the homogeneity tolerance $m = 20$.

The adaptive GANMM-based approach overcomes the usual non-adaptive MM-based one, achieving a much better segmentation of the original image, with the visually expected result reached for $m = 20$. Indeed, these connected GAN filters do not damage the grain boundaries and well smooth the image inside the grains, contrary to those usual non-adaptive ones.

**Remark 7.** *Therefore, the minima of the adaptively filtered image provide significant markers, necessary to the watershed process.*

### *3.6. Segmentation in Uneven Illumination Conditions*

The main aim of this subsection is to practically put in evidence the physical irrelevance of the $CLIP$ framework. It is illustrated on the previous metallurgic image where the segmentation in uneven illumination conditions is not robustly achieved within the CLIP framework. Precisely, image segmentation in presence of a locally small change in scene illumination is robustly addressed by the $LIP$ approach, contrary to the $CLIP$ one (Fig. 8).
To simulate the small change in scene illumination, the original image $f$ has been modified in three steps, to produce $\check{f}$ (Fig. 7):

1. the original image $f$ is first inverted: $\overline{f} = M - f$, where $M$ is the supremum of the range where images are digitized and stored,
2. $\overline{f}$ is then lightened gradually from left to right using a multiplicative lightening function $I_{lt}$ [27] defined by:

$$\forall (x,y) \in D \quad I_{lt}(x,y) \;=\; \left(1 - 0.8\left(1 - \cos\left(\frac{\pi}{2} \times \frac{x}{256}\right)\right)\right) \tag{9}$$

   where $(x, y)$ denotes the point coordinates.
   So, $g = I_{lt} \times \overline{f}$ ,
3. the image $g$ is finally inverted to produce the resulting image: $\check{f} = \overline{g} = M - g$.

The transformation $g = I_{lt} \times \overline{f}$ is in accordance with the multiplicative reflectance and transmittance image formation models [72, 44].
In practice, the original image and the non-uniformly lightened image are exposed in Figure 7.

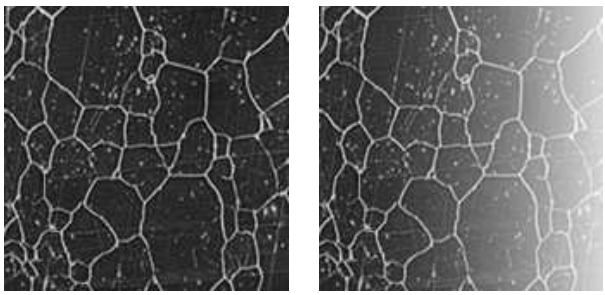

a. original $f$ b. non-uniformly lightened $\check{f}$

*Figure 7.* Simulation of a locally small change in scene illumination: original [a] image, and a non-uniformly lightened [b] image obtained by (8).

The segmentation (the same process applied in the precedent subsection 3.5) of the image $\check{f}$ is compared from ASEs (Eq. 34 in [20]) built in the CLIP and LIP frameworks [20] selected for the space of criterion mappings, denoted respectively $\mathcal{C}_{CLIP}$ and $\mathcal{C}_{LIP}$.

The resulting segmentation generated within the LIP framework is far better. Indeed, the process fails to detect boundaries in the overlighted areas of the lightened image within the CLIP framework. The process $Wat(\mathrm{CO}^{\check{f}}_{23_{\triangle}}(\check{f}))$ in $\mathcal{C}_{LIP}$ supplies, from a visual inspection, the expected segmentation. This experimental results highlight the $LIP$ approach since it is physically connected to the human visual system and the perceptual notions of contrast [42, 73].

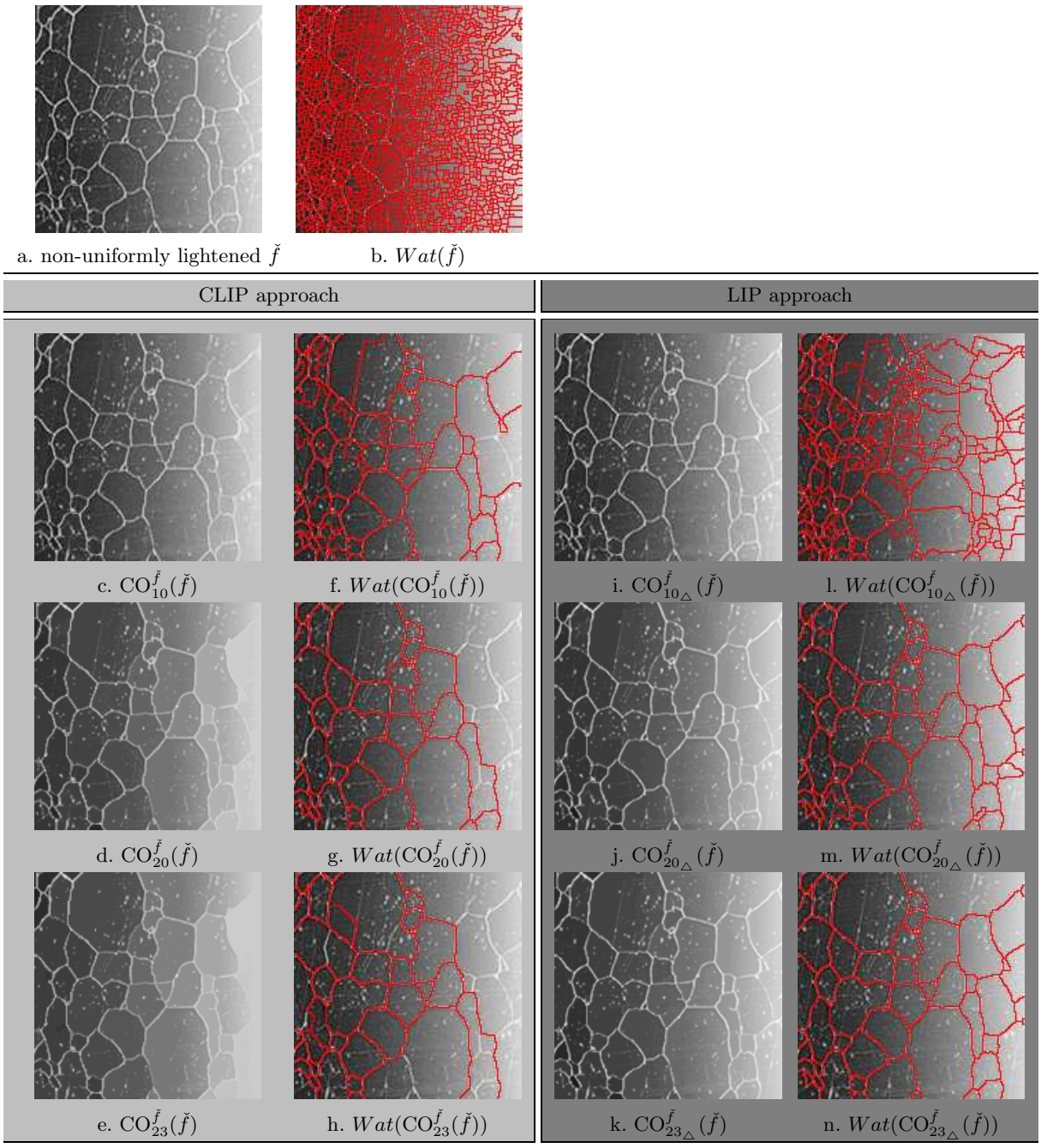


*Figure 8.* GANIP-based segmentation of a real metallurgic grain boundaries [a] image in uneven illumination conditions. The original image is first decomposed with adaptive closing-openings performed in $\mathcal{C}_{CLIP}$ [c-e] and $\mathcal{C}_{LIP}$ [i-k] frameworks selected for the space of criterion mappings. Finally, the watershed transform, denoted $Wat$ is completed on this segmentation function, achieving the images [f-h] and [l-n], for the respective CLIP and LIP approaches. The LIP technique robustly achieves the segmentation, in the sense that the process $Wat(\mathrm{CO}^{\check{f}}_{23}(\check{f}))$ generates almost the same partition as $Wat(\mathrm{CO}^{f}_{20}(f))$ in standard illumination conditions (Fig. 6).

## 4. Image Enhancement

Image enhancement is the improvement of image quality, wanted e.g. for visual inspection or for machine analysis. Physiological experiments have shown that very small changes in luminance

are recognized by the human visual system in regions of continuous gray tones, and not at all seen in regions of some discontinuities [100]. Therefore, a design goal for image enhancement is often to smooth images in more uniform regions, but to preserve edges. On the other hand, it has also been shown that somehow degraded images with enhancement of certain features, e.g. edges, can simplify image interpretation both for a human observer and for machine recognition [100]. A second design goal, therefore, is image sharpening [31].

In this paper, the considered image enhancement process is edge sharpening: the approach is similar with unsharp masking [77] type enhancement where a highpass portion is added to the original image. The contrast enhancement process is realized through the *toggle contrast* [96], whose operator $\kappa_r$ is defined as following:

**Definition 8 (Toggle Contrast).**
$\forall (f, x, r) \in \mathcal{I} \times D \times \mathbb{R}^+$

$$\kappa_r(f)(x) = \begin{cases} \mathrm{D}_r(f)(x) & \textit{if } \mathrm{D}_r(f)(x) - f(x) < f(x) - \mathrm{E}_r(f)(x) \\ \mathrm{E}_r(f)(x) & \textit{otherwise} \end{cases} \tag{10}$$

*where* $\mathrm{D}_r$ *and* $\mathrm{E}_r$ *denote respectively the classical dilation and erosion (Eq. 29 and 30 in [20]), using a disk of radius* $r$ *as SE.*

At each point $x$, the output value of this filter toggles between the value of the dilation of $f$ by $B$ (i.e., the maximum of $f$ inside the operational window $B$ centered) at $x$ and the value of its erosion by $B$ (i.e., the minimum of $f$ within the same window) according to which is closer to the input value $f(x)$.

Figure 9 illustrates a one-dimensional example of the toggle contrast operator.

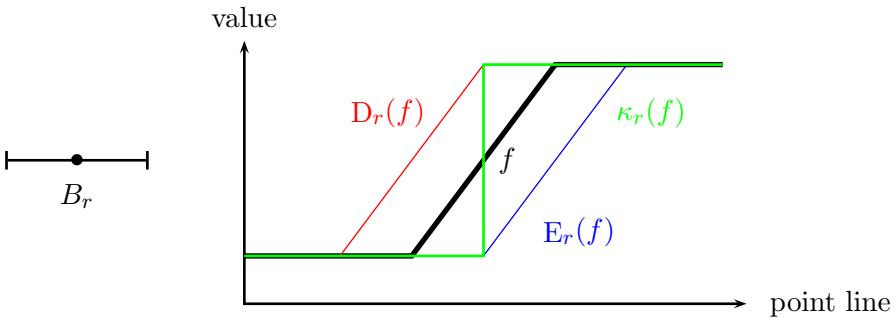


*Figure 9.* One-dimensional representation of the toggle contrast operator. For a point $x$ of $f$, the value of the resulting filter $\kappa_r(f)(x)$ toggles between the value $\mathrm{D}_r(f)(x)$ and the value $\mathrm{E}_r(f)(x)$, using the centered disk $B_r$ of radius $r$.

This non-adaptive toggle contrast is extended through the GANIP approach with adaptive dilation and erosion (Eq. 35-38 in [20]). Using a 'contrast' criterion within the definition of ASEs, which is naturally adapted to that edge sharpening transformation, it leads to the *adaptive toggle contrast* (Def. 10). This transformation requires a 'contrast' definition introduced in the digital setting of the LIP framework [45] (see [70, 71] for the continuous setting):

**Definition 9 (LIP Contrast).**
*The LIP contrast at a point $x \in D$ of an image $f \in \mathcal{I}$, denoted $C(f)(x)$, is defined with the help of its neighbors included in a disk $V(x)$ of radius 1, centered in $x$:*

$$C(f)(x) = \frac{1}{\#V(x)} \barwedge \bigbarwedge_{y \in V(x)} (\max(f(x), f(y)) \barwedge \min(f(x), f(y))) \tag{11}$$

*where $\bigbarwedge$ and $\#$ denote the sum in the LIP sense, and the cardinal symbol, respectively.*

Consequently, the so-called adaptive toggle contrast is the transformation $\kappa_{m_\triangle}^{C(f)}$, where $C(f)$ and $m_\triangle$ denotes respectively the 'contrast' criterion mapping and the homogeneity tolerance within the LIP framework (required for the GANs definition):

**Definition 10 (Adaptive Toggle Contrast).**
$\forall (f, x, m_\triangle) \in \mathcal{I}_{CLIP} \times D \times E_{m_\triangle}$

$$\kappa_{m_\triangle}^{C(f)}(f)(x) = \begin{cases} \mathrm{D}_{m_\triangle}^{C(f)}(f)(x) & \textit{if } \mathrm{D}_{m_\triangle}^{C(f)}(f)(x) - f(x) < f(x) - \mathrm{E}_{m_\triangle}^{C(f)}(f)(x) \\ \mathrm{E}_{m_\triangle}^{C(f)}(f)(x) & \textit{otherwise} \end{cases} \tag{12}$$

*where $\mathrm{D}_m^{C(f)}$ and $\mathrm{E}_m^{C(f)}$ (Eq. 35-38 in [20]) denote respectively the adaptive dilation and adaptive erosion, using ASEs computed on the criterion mapping $C(f)$ with the homogeneity tolerance $m_\triangle$ (Eq. 5).*

Figure 10 exposes two illustration examples of image enhancement using respectively classical and adaptive toggle contrast. The process is both applied on the 'Lena' image, and on a real image acquired on the retina of a human eye.

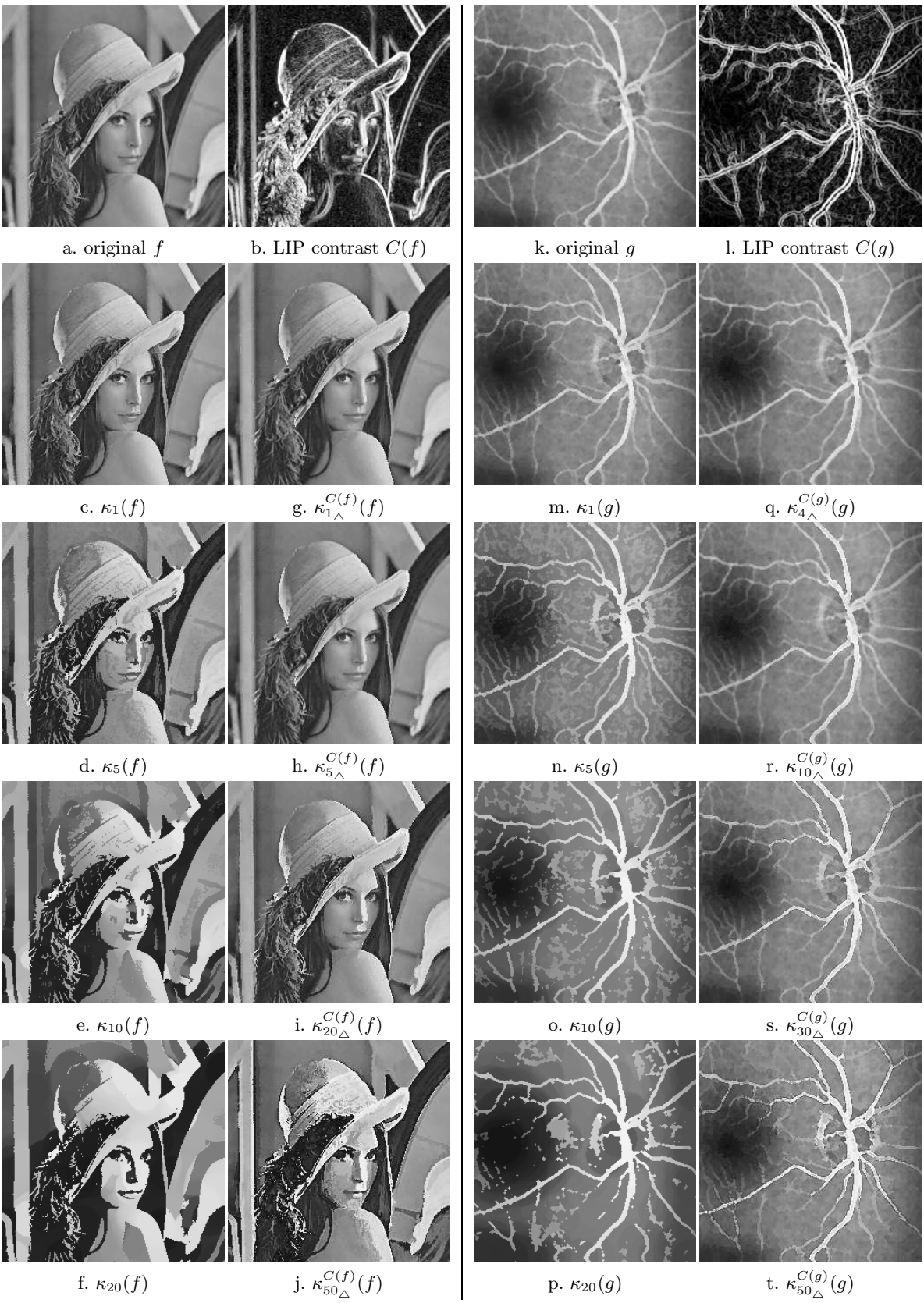


*Figure 10.* Two illustration examples of image enhancement using the toggle contrast process. The operator is both applied on 'Lena' [a] image, and on a real [k] image acquired on the retina of a human eye. The enhancement is achieved with the usual toggle contrast [c-f, m-p] and the GANIP-based toggle contrast [g-j, q-t] using the LIP contrast criterion [b,l]. Using the usual toggle contrast, the edges are disconnected as soon as the filtering becomes too strong. On the contrary, such structures are preserved and sharpened with the adaptive filters.

This image enhancement example confirms that the GANIP-based operators are more effective than the corresponding usual ones. Indeed, the adaptive toggle LIP contrast performs a locally accurate image enhancement, taking into account the notion of contrast within spatial structures of the image. Consequently, only the transitions are sharpened while preserving the homogeneous regions. On the contrary, the usual toggle contrast enhances the image in a uniform way. Thus, the spatial zones around transitions are rapidly damaged as soon as the filtering becomes too strong.

## 5. Conclusion and Prospects

This Part II aimed to present some practical application examples of the General Adaptive Neighborhood Image Processing (GANIP) approach, whose theoretical aspects have been exposed in [20]. Several fields of image processing have been investigated, such as image filtering, image segmentation and image enhancement. In this paper, the GANIP approach has been more particularly used in the context of Mathematical Morphology (MM). In several and practical cases, it supplies connected operators, which is of great morphological and topological importance. The resulting adaptive morphological operators perform a significant spatially-adaptive processing, taking into account the local characteristics of the image, thanks to the analyzing criterion. For instance, the notion of contrast allows efficient image enhancement (Section 4). In addition, the use of general linear image processing frameworks enables a connection with the physical and/or physiological image settings. For example, the LIP framework has been necessary in uneven illumination conditions (Section 3.6).

Finally, the General Adaptive Neighborhood Image Processing approach opens new pathways that promise large prospects in several fields of image processing. The authors are interested in putting into practice processes based on other analyzing criteria, such as curvature, thickness, orientation, ... Moreover, the application of topological concepts and tools, using the GAN paradigm, should allow image features to be more significantly analyzed.

## Acknowledgments

The authors wish to thank their colleague Y. Gavet (ENSM.SE/CIS) for his encouragement and his computing contributions.

## References

1. L. Alvarez, F. Guichard, P.L. Lions, and J.M. Morel, "Axioms and fundamental equations in image processing," *Arch. for Rational Mechanics*, Vol. 123, pp. 199–257, 1993.
2. G.R. Arce and R.E. Foster, "Detail-Preserving ranked-order based filters for image processing," *IEEE Transactions on Acoustics, Speech, and Signal Processing*, Vol. 37, No. 1, pp. 83–98, 1989.
3. J. Astola and P. Kuosmanen, *Fundamentals of Nonlinear Digital Filtering*, CRC Press: Boca Raton, New York, U.S.A., 1997.
4. S. Beucher and C. Lantuejoul, "Use of watersheds in contour detection," in *International Workshop on image processing, real-time edge and motion detection/estimation*, Rennes, France, 1979, .
5. S. Beucher and F. Meyer, "The morphological approcah to segmentation: the watershed transformation," in *Mathematical Morphology in Image Processing*, E. Dougherty (Ed.), N.Y., U.S.A., 1993, pp. 433–481.
6. U.d.M. Braga Neto, "Alternating Sequential Filters by Adaptive-Neighborhood Structuring Functions," in *Mathematical Morphology and its Applications to Image and Signal Processing*, P. Maragos, R. W. Schafer, and M. A. Butt (Eds.), 1996, pp. 139–146.

7. J.C. Brailean, B.J. Sullivan, C.T. Chen, and M.L. Giger, "Evaluating the EM algorithm for image processing using a human visual fidelity criterion," in *Proceedings of the International Conference on Acoustics, Speech and Signal Processing*, 1991, pp. 2957–2960.
8. V. Buzuloiu, M. Ciuc, R.M. Rangayyan, and C. Vertan, "Adaptive-Neighborhood Histogram Equalization of Color Images," *Electronic Imaging*, Vol. 10, No. 2, pp. 445–459, 2001.
9. E. Cech, *Topological Spaces*, John Wiley & Sons Ltd.: Prague, Czechoslovakia, 1966.
10. M. Charif-Chefchaouni and D. Schonfeld, "Spatially-Variant Mathematical Morphology," in *Proceedings of the IEEE International Conference on Image Processing*, 1994, . Austin, Texas, U.S.A.; November, 13-16.
11. J.C. Chazallon, L.and Pinoli, "An Automatic Morphological Method for Aluminium Grain Segmentation in Complex Grey Level Images," *Acta Stereologica*, Vol. 16, No. 2, pp. 119–130, 1997.
12. G. Choquet, *Topology*, Academic Press: New-York, U.S.A., 1966.
13. G. Choquet, *Cours de topologie*, chapt. Espaces topologiques et espaces métriques, pp. 45–51, Dunod: Paris, France, 2000.
14. M. Ciuc, "Traitement d'images multicomposantes : application à l'imagerie couleur et radar," Ph.D. thesis, Université de Savoie - Université Polytechnique de Bucarest, Roumanie, 2002.
15. M. Ciuc, R.M. Rangayyan, T. Zaharia, and V. Buzuloiu, "Filtering Noise in Color Images using Adaptive-Neighborhood Statistics," *Electronic Imaging*, Vol. 9, No. 4, pp. 484–494, 2000.
16. J. Crespo, J. Serra, and R.W. Schafer, "Theoretical aspects of morphological filters by reconstruction," *Signal Processing*, Vol. 47, pp. 201–225, 1995.
17. O. Cuisenaire, "Locally Adaptable Mathematical Morphology," in *Proceedings of the IEEE International Conference on Image Processing*, 2005, . Genova, Italy; September, 11-14.
18. S.C. Dakin and R.F. Hess, "The Spatial Mechanisms Mediating Symmetry Perception," *Vision Research*, Vol. 37, pp. 2915–2930, 1997.
19. J. Debayle, "General Adaptive Neighborhood Image Processing," Ph.D. thesis, Ecole Nationale Supérieure des Mines, Saint-Etienne, France, 2005.
20. J. Debayle and J.C. Pinoli, "General Adaptive Neighborhood Image Processing - Part I: Introduction and Theoretical Aspects," *Journal of Mathematical Imaging and Vision*, submitted paper.
21. J. Debayle and J.C. Pinoli, "General Adaptive Neighborhood Image Processing - Part II: Practical Application Examples," *Journal of Mathematical Imaging and Vision*, submitted paper.
22. J. Debayle and J.C. Pinoli, "Adaptive-Neighborhood Mathematical Morphology and its Applications to Image Filtering and Segmentation," in *9th European Congress on Stereology and Image Analysis*, Zakopane, Poland, 2005a, pp. 123–130.
23. J. Debayle and J.C. Pinoli, "Multiscale Image Filtering and Segmentation by means of Adaptive Neighborhood Mathematical Morphology," in *Proceedings of the IEEE International Conference on Image Processing*, Genova, Italy, 2005b, pp. 537–540.
24. J. Debayle and J.C. Pinoli, "Spatially Adaptive Morphological Image Filtering using Intrinsic Structuring Elements," *Image Analysis and Stereology*, Vol. 24, No. 3, pp. 145–158, 2005c.
25. G. Deng and L.W. Cahill, "Multiscale image enhancement using the logarithmic image processing model," *Electronic Letters*, Vol. 29, pp. 803–804, 1993.
26. G. Deng, L.W. Cahill, and J.R. Tobin, "A study of the logarithmic image processing model and its application to image enhancement," *IEEE Transactions on Image Processing*, Vol. 4, pp. 506–512, 1995.
27. G. Deng and J.C. Pinoli, "Differentiation-Based Detection Using the Logarithmic Image Processing Model," *Journal of Mathematical Imaging and Vision*, Vol. 8, pp. 161–180, 1998.
28. G. Deng, J.C. Pinoli, W.Y. Ng, L.W. Cahill, and M. Jourlin, "A comparative study of the Log-ratio image processing approach and the logarithmic image processing model," unpublished manuscript, 1994.
29. E.R. Dougherty and J. Astola, *An introduction to nonlinear image processing*, SPIE Press: Bellingham, 1994.
30. N. Dunford and J.T. Schwartz, *Linear Operators, Part I, General Theory*, Wiley-Interscience: New-York, U.S.A., 1988.
31. R.C. Gonzalez and R.E. Woods, *Digital Image Processing*, Addison-Wesley, 1992.
32. R. Gordon and R.M. Rangayyan, "Feature Enhancement of Mammograms using Fixed and Adaptive Neighborhoods," *Applied Optics*, Vol. 23, No. 4, pp. 560–564, 1984.
33. D.J. Granrath, "The role of human visual models in image processing," in *Proceedings of the IEEE*, 1981, pp. 552–561.
34. P. Gremillet, M. Jourlin, and J.C. Pinoli, "LIP model-based three-dimensionnal reconstruction and visualisation of HIV infected entire cells," *Journal of Microscopy*, Vol. 174, pp. 31–38, 1994.
35. M. Grimaud, "La géodésie numérique en morphologie mathématique. Application à la détection automatique de microcalcifications en mammographie numérique," Ph.D. thesis, Ecole Nationale Supérieure des Mines de Paris, France, 1991.
36. J.E. Hafstrom, *Introduction to Analysis and Abstract Algebra*, W.B. Saunders: Philadelphia, U.S.A., 1967.
37. P. Hawkes, "Image Algebra and Rank-Order Filters," *Scanning Microscopy*, Vol. 11, pp. 479–482, 1997.

38. H.J.A.M. Heijmans and R.V.D. Boomgaard, "Algebraic Framework for Linear and Morphological Scale-Spaces," *Journal of Visual Communication and Image Representation*, Vol. 13, No. 1/2, pp. 269–301, 2000.
39. A.K. Jain, "Advances in mathematical models for image processing," in *Proceedings of the IEEE*, 1981, pp. 502–528.
40. K. Jänich, *Topology*, Springer: Berlin, Germany, 1983.
41. M. Jourlin and J.C. Pinoli, "Logarithmic Image Processing," *Acta Stereologica*, Vol. 6, pp. 651–656, 1987.
42. M. Jourlin and J.C. Pinoli, "A model for logarithmic image processing," *Journal of Microscopy*, Vol. 149, pp. 21–35, 1988.
43. M. Jourlin and J.C. Pinoli, "Image dynamic range enhancement and stabilization in the context of the logarithmic image processing model," *Signal Processing*, Vol. 41, pp. 225–237, 1995.
44. M. Jourlin and J.C. Pinoli, "Logarithmic Image Processing : The Mathematical and Physical Framework for the Representation and Processing of Transmitted Images," *Advances in Imaging and Electron Physics*, Vol. 115, pp. 129–196, 2001.
45. M. Jourlin, J.C. Pinoli, and R. Zeboudj, "Contrast definition and contour detection for logarithmic images," *Journal of Microscopy*, Vol. 156, pp. 33–40, 1988.
46. L Kantorovitch and G. Akilov, *Analyse Fonctionnelle*, Editions Mir: Moscou, Russia, 1981.
47. J.L. Kelley, *General Topology*, D. Van Nostrand: New-York, U.S.A., 1955.
48. S. Lang, *Linear Algebra*, Addison Wesley, Reading, MA, 1966.
49. G. Laporterie, F.and Flouzat and O. Amram, "The Morphological Pyramid and its Applications to Remote Sensing : Multiresolution Data Analysis and Features Extraction," *Image Analysis and Stereology*, Vol. 21, No. 1, pp. 49–53, 2002.
50. J.S. Lee, "Refined Filtering of Image using Local Statistics," *Computer Graphics and Image Processing*, Vol. 15, pp. 380–389, 1981.
51. R Lerallut, E Decencire, and F. Meyer, "Image filtering using morphological amoebas," in *Proceedings of the 7th International Symposium on Mathematical Morphology*, C. Ronse, L. Najman, and E. Decencire (Eds.), Paris, France, 2005, pp. 13–22.
52. J.S. Lim, *Two-Dimensional Signal and Image Processing*, Prentice-Hall: Englewood Cliffs, New-Jersey, U.S.A., 1990.
53. T. Lindeberg, "Scale-Space Theory: a Basic Tool for Analysing Structures at Different Scales," *Journal of Applied Statistics*, Vol. 21, No. 2, pp. 225–270, (Supplement on Advances in Applied Statistics: Statistics and Images: 2)., 1994.
54. W.A.J. Luxemburg and A.C. Zaanen, *Riesz Spaces*, North Holland: Amsterdam, Netherlands, 1971.
55. S.G. Mallat, "A Theory for Multiresolution Decomposition : The Wavelet Representation," *IEEE Transactions on Pattern Analysis and Machine Intelligence*, Vol. 11, pp. 674–693, 1989.
56. P.A. Maragos and R.W. Schafer, "Morphological filters, Part I: Their set-theoretic analysis and relations to linear shift invariant filters," *IEEE Transactions on Acoustics, Speech and Signal Processing*, Vol. 35, No. 8, pp. 1153–1169, 1987a.
57. P.A. Maragos and R.W. Schafer, "Morphological filters, Part II: Their relations to median order statistic, and stack filters," *IEEE Transactions on Acoustics, Speech and Signal Processing*, Vol. 35, No. 8, pp. 1170–1184, 1987b.
58. D. Marr, *Vision: A Computational Investigation into the Human Representation and Processing of Visual Information*, W.H. Freeman and Company: San Fransisco, U.S.A., 1982.
59. G. Matheron, *Eléments pour une théorie des milieux poreux*, Masson: Paris, 1967.
60. G. Matheron, *Image Analysis and Mathematical Morphology. Volume 2 : Theoretical Advances*, chapt. Filters and Lattices, pp. 115–140, Academic Press: London, U.K., 1988.
61. F. Mayet, J.C. Pinoli, and M. Jourlin, "Justifications physiques et applications du modèle LIP pour le traitement des images obtenues en lumière transmise," *Traitement du signal*, Vol. 13, pp. 251–262, 1996.
62. F. Meyer and S. Beucher, "Morphological Segmentation," *Journal of Visual Communication and Image Representation*, Vol. 1, No. 1, pp. 21–46, 1990.
63. M. Nagao and T. Matsuyama, "Edge preserving Smoothing," *Computer Graphics and Image Processing*, Vol. 9, pp. 394–407, 1979.
64. A.V. Oppenheim, "Superposition in a class of nonlinear systems," Research Laboratory of Electronics, M.I.T., Cambridge, U.S.A., Technical report, 1965.
65. A.V. Oppenheim, "Generalized Superposition," *Information and Control*, Vol. 11, pp. 528–536, 1967.
66. A.V. Oppenheim, "Nonlinear filtering of Multiplied and Convolved Signals," in *Proceedings of the IEEE*, 1968, .
67. R.B. Paranjape, R.M. Rangayyan, and W.M. Morrow, "Adaptive Neighbourhood Mean and Median Image Filtering," *Electronic Imaging*, Vol. 3, No. 4, pp. 360–367, 1994.
68. P. Perona and J. Malik, "Scale-Space and Edge Detection using Anisotropic Diffusion," *IEEE Transactions on Pattern Analysis and Machine Intelligence*, Vol. 12, No. 7, pp. 629–639, 1990.

69. J.C. Pinoli, "Contribution à la modélisation, au traitement et à l'analyse d'image," Ph.D. thesis, Department of Mathematics, University of Saint-Etienne, France, 1987.
70. J.C. Pinoli, "A contrast definition for logarithmic images in the continuous setting," *Acta Stereologica*, Vol. 10, pp. 85–96, 1991.
71. J.C. Pinoli, "Modélisation et traitement des images logarithmiques: Théorie et applications fondamentales," Department of Mathematics, University of Saint-Etienne, Technical Report 6 (this report is a revised and expanded synthesis of the theoretical basis and several fundamental applications of the LIP approach published from 1984 to 1992. It has been reviewed by international referees and presented in December 1992 for passing the "Habilitation à Diriger des Recherches" French degree), 1992.
72. J.C. Pinoli, "A General Comparative Study of the Multiplicative Homomorphic, Log-Ratio and Logarithmic Image Processing Approaches," *Signal Processing*, Vol. 58, pp. 11–45, 1997a.
73. J.C. Pinoli, "The Logarithmic Image Processing Model : Connections with Human Brightness Perception and Contrast Estimators," *Journal of Mathematical Imaging and Vision*, Vol. 7, No. 4, pp. 341–358, 1997b.
74. I. Pitas and A.N. Venetsanopoulos, *Nonlinear Digital Filters: Principles and Applications*, Kluwer Academic: Norwell Ma., U.S.A., 1990.
75. I. Pitas and A.N. Venetsanopoulos, "Order statistics in digital image processing," in *Proceedings of the IEEE*, 1992, pp. 1893–1923.
76. T.F. Rabie, R.M. Rangayyan, and R.B. Paranjape, "Adaptive-Neighborhood Image Deblurring," *Electronic Imaging*, Vol. 3, No. 4, pp. 368–378, 1994.
77. G. Ramponi, N. Strobel, S.K. Mitra, and T.H. Yu, "Nonlinear Unsharp Masking Methods for Image-Contrast Enhancement," *Journal of Electronic Imaging*, Vol. 5, No. 3, pp. 353–366, 1996.
78. R.M. Rangayyan, M. Ciuc, and F. Faghih, "Adaptive-Neighborhood Filtering of Images corrupted by Signal-Dependent Noise," *Applied Optics*, Vol. 37, No. 20, pp. 4477–4487, 1998.
79. R.M. Rangayyan and A. Das, "Filtering Multiplicative Noise in Images using Adaptive Region-Based Statistics," *Electronic Imaging*, Vol. 7, No. 1, pp. 222–230, 1998.
80. G.X. Ritter, "Recent developments in image algebra," in *Advances in Electronics and Electron Physics*, P. Hawkes (Ed.), New-York, U.S.A., 1991, pp. 243–308.
81. G.X. Ritter and J.N. Wilson, *Handbook of Computer Vision Algorithms in Image Algebra*, CRC Press: Boca Ration, FL, U.S.A., 1996.
82. G.X. Ritter, J.N. Wilson, and J.L. Davidson, "Image algebra, an overview," *Computer Vision, Graphics, and Image Processing*, Vol. 49, No. 3, pp. 297–331, 1990.
83. M. Ropert and D. Pelé, "Synthesis of Adaptive Weighted Order Statistic Filters with Gradient Algorithms," in *Mathematical Morphology and its Applications to Image Processing*, J. Serra and P. Soille (Eds.), 1994, pp. 37–44.
84. A. Rosenfeld, *Picture Processing by Computers*, Academic Press: New-York, U.S.A., 1969.
85. P. Salembier, "Structuring Element Adaptation for Morphological Filters," *Journal of Visual Communication and Image Representation*, Vol. 3, No. 2, pp. 115–136, 1992.
86. P. Salembier and J. Serra, "Flat zones filtering, connected operators, and filters by reconstruction," *IEEE Transactions on Image Processing*, Vol. 4, No. 8, pp. 1153–1159, 1995.
87. W.F. Schreiber, *Fundamentals of Electronic Imaging Systems: Some Aspects of Image Processing*, Springer: Berlin, Germany2nd. ed. edition, 1991.
88. J. Serra, "L'analyse des textures par la géométrie aléatoire," Comptes-Rendus du Comité Scientifique de l'IRSID, 1965.
89. J. Serra, *Image Analysis and Mathematical Morphology*, Academic Press: London, U.K., 1982.
90. J. Serra, *Image Analysis and Mathematical Morphology. Volume 2 : Theoretical Advances*, chapt. Mathematical Morphology for Complete Lattices, pp. 13–35, Academic Press: London, U.K., 1988a.
91. J. Serra, *Image Analysis and Mathematical Morphology. Volume 2 : Theoretical Advances*, chapt. Alternating Sequential Filters, pp. 203–216, Academic Press: London, U.K., 1988b.
92. J. Serra, *Image Analysis and Mathematical Morphology. Volume 2 : Theoretical Advances*, chapt. Introduction to Morphological Filters, pp. 101–114, Academic Press: London, U.K., 1988c.
93. J. Serra and P. Salembier, "Connected Operators and Pyramids," in *Proceedings of SPIE*, San Diego, U.S.A., 1993, pp. 65–76.
94. H. Shvayster and S. Peleg, "Pictures as elements in a vector space," in *Proceedings of the IEEE International Conference on Computer Vision and Pattern Recognition*, Washington, U.S.A., 1983, pp. 442–446.
95. H Shvayster and S. Peleg, "Inversion of Picture Operators," *Pattern Recognition Letters*, Vol. 5, pp. 49–61, 1987.
96. P. Soille, *Morphological Image Analysis. Principles and Applications*, chapt. Filtering, pp. 241–266, Springer Verlag: New York, 2003a.
97. P. Soille, *Morphological Image Analysis. Principles and Applications*, chapt. Introduction, pp. 1–14, Springer Verlag: New York, 2003b.

98. W.J. Song and W.A. Pearlman, "Restoration of Noisy Images with Adaptive Windowing and Nonlinear Filtering," in *Visual Communication and Image Processing*, 1986, pp. 198–206.
99. T.G. Stockham, "The applications of generalized linearity to automatic gain control," *IEEE Transactions on Audio and Electroacoustics*, Vol. AU-16, No. 2, pp. 267–270, 1968.
100. T.G. Stockham, "Image Processing in the Context of a Visual Model," in *Proceedings of the IEEE*, 1972, pp. 825–842.
101. G. Strang, *Linear Algebra and its Applications*, Academic Press: New-York, U.S.A., 1976.
102. F.K. Sun and P. Maragos, "Experiments on Image Compression using Morphological Pyramids," in *Proceedings of the SPIE Visual Communications and Image Processing*, 1989, pp. 1303–1312.
103. C. Vachier, "Morphological Scale-Space Analysis and Feature Extraction," in *Proceedings of the IEEE International Conference on Image Processing*, Thessaloniki, Greece, 2001, pp. 676–679.
104. F.A. Valentine, *Convex Sets*, McGraw-Hill: New-York, U.S.A., 1964.
105. J.G. Verly and R.L. Delanoy, "Some Principles and Applications of Adaptive Mathematical Morphology for Range Imagery," *Optical Engineering*, Vol. 32, No. 12, pp. 3295–3306, 1993.
106. L. Vincent and P. Soille, "Watersheds in Digital Spaces: An Efficient Algorithm based on Immersion Simulations," *IEEE Transaction on Pattern Analysis and Machine Intelligence*, Vol. 13, No. 6, pp. 583–589, 1991.
107. R.C. Vogt, "A Spatially Variant, Locally Adaptive, Background Normalization Operator," in *Mathematical Morphology and its Applications to Image Processing*, J. Serra and P. Soille (Eds.), 1994, pp. 45–52.
108. M. Wertheimer, *A sourcebook of Gestalt Psychology*, chapt. Laws of Organization in Perceptual Forms, pp. 71–88, Hartcourt, Brace, 1938.